An efficient model for underwater noise prediction during pile driving ⊘

Rui He ⓘ ; Yongshan Song

Check for updates

View Online

Export Citation

Articles You May Be Interested In
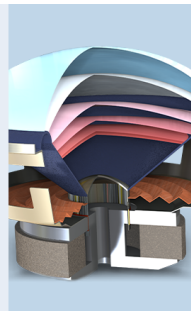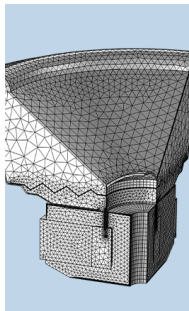
Sound radiation from impact-driven raked piles

J. Acoust. Soc. Am. (July 2017)

A fast computational model for near- and far-field noise prediction due to offshore pile driving

J. Acoust. Soc. Am. (March 2021)

Modeling the noise mitigation of a bubble curtain

J. Acoust. Soc. Am. (October 2019)

JASA ARTICLE

An efficient model for underwater noise prediction during pile driving

Rui He[a] [iD] and Yongshan Song

College of Harbor, Coastal and Offshore Engineering, Hohai University, Nanjing 210024, China

ABSTRACT:

Underwater noise pollution from pile driving is now attracting increasing attention. However, most of the current numerical and semi-analytical models for predicting the noise are still expensive and time-consuming, and the near-field noise and far-field noise have to be obtained from different models. This paper proposes an efficient semi-analytical solution for predicting underwater noise in both near field and far field with only one model, whose computational efficiency is orders of magnitude higher than that of the finite element model. It is the first time that the Baranov–Novak thin-layer model for soil-pile interaction has been extended to the subject of underwater noise prediction during pile installation, taking into account pile-fluid-soil interaction. The solutions are obtained using the Laplace transform and the variable separation method. By comparing the prediction results with the five reported research cases, it is shown that the error of the proposed model is within reasonable limits for both near-field and far-field noise predictions. © *2024 Acoustical Society of America.* https://doi.org/10.1121/10.0028128

(Received 1 December 2023; revised 2 July 2024; accepted 7 July 2024; published online 7 August 2024)

[Editor: Stephen P. Robinson]   Pages: 774–782

I. INTRODUCTION

In developing and constructing offshore wind farms (OWFs), reports indicate that the vibration and noise generated by pile driving pose a potential threat to marine mammals.[1–3] Field measurements have shown that high-amplitude impulsive noise from pile driving can lead to hearing loss in marine animals and fish.[4] In addition, pile driving noise dissipates slowly in the ocean and can be detected more than 10 km from the pile.[5] To protect the marine ecosystem, reasonable predictions of vibration and noise levels caused by pile driving have become a hot research topic in recent years.

Over the past few decades, numerical models [e.g., finite element method (FEM)[6,7] or finite difference method[8]] have been the main methods used to study the near-field noise generated by offshore pile driving. Due to limited computing power and high computational costs, numerical models are usually used to model the near-field underwater noise.

For far-field underwater noise prediction, the long-range methods (e.g., the parabolic equation method,[9,10] wave-number integration method,[11] and normal mode method[12]) are combined with sound generation models. By simplifying the seabed as an acoustic medium, Reinhall and Dahl[13] first systematically investigated the generation and propagation of underwater noise caused by impact pile driving. It was found that the underwater noise was mainly caused by the radial expansion of the pile, and Mach cone-shaped sound pressure fields were observed. Lippert and von Estorff[14] analyzed the influence of soil parameters on the results and showed that simplifying the soil as an

acoustic medium may lead to some errors. The seabed was then assumed to be an elastic medium.[15,16] Compared to the acoustic medium model, the contribution of shear waves in the soil and the effect of Scholte waves along the seawater-seabed interface can be considered in the elastic model. Recently, He *et al.*[17] proposed a poroelastic model for the near-field underwater noise caused by pile driving, which can better account for the pile driving noise in soils with partially drained conditions, and the sound attenuation effect of the seabed can also be well evaluated.

Since purely numerical methods are too computationally intensive, semi-analytical models are then developed to investigate the underwater noise from pile driving. Hall[18] obtained the radiated sound pressure from offshore pile driving by linking the radial displacement of the pile to a sound radiation model. A complete coupled offshore pile driving system was proposed by Tsouvalas and Metrikine,[19] which included the hydraulic hammer, the pile, and the fluid, while the seabed was assumed to be linear springs and dashpots. The vibration of the pile was described by thin-shell theory, and the response of the system was solved semi-analytically using the modal matching technique. Deng *et al.*[20] also presented a semi-analytical model based on the variational method by simplifying the soil as springs and dashpots. The spring models had high computational speed for sound prediction, but the spring and dashpot coefficients are difficult to determine accurately in practice. Subsequently, Tsouvalas and Metrikine[21,22] developed a pile-fluid-soil interaction model in which the seabed was modelled as a three-dimensional (3D) layered elastic medium, and the model was extended to include far-field noise prediction by coupling the sound generation module with the sound propagation module.[23] As the method involves infinite integrals

[a]Email: herui@hhu.edu.cn

TABLE I. Differences between the existing models and this analytical model.

Existing methods	The differences
Numerical models (Refs. 6–17)	Compared to numerical methods, the simplified semi-analytical model is more computationally efficient.
	The far-field sound prediction needs long-range modules in the numerical models, whereas it can be obtained directly by this model.
Semi-analytical model: the seabed is simplified as fluid medium (Ref. 18).	The soil in Ref. 18 is assumed to be an acoustic medium, but is considered as an elastic medium in this model.
Semi-analytical model: the seabed is simplified as springs and dashpots (Refs. 19 and 20).	It is difficult to accurately estimate the spring and dashpot constants in these semi-analytical models, which can be avoided in this model.
Semi-analytical model: the seabed is assumed to be elastic medium (Refs. 21–23).	The method in Refs. 21–23 is a modal matching technique that involves searching for eigenfrequencies and eigenmodes, and it needs to handle the infinite integrals with several poles, which makes the calculation complex. The simplified semi-analytical model based on Novak's method avoids these difficulties.

and poles, the accurate numerical calculation is quite complex.

To develop a simplified and quick prediction model of underwater noise caused by pile driving, an axisymmetric pile-fluid-soil interaction model is established based on some simplified assumptions similar to the Baranov–Novak model,[24] which is widely used in pile-soil dynamics due to its simplicity and efficiency. The dynamic governing equations are obtained and solved in the frequency domain using the Laplace transform and the variable separation method. Combining the boundary conditions, analytical solutions of the pile displacements and the fluid pressure are obtained. It can predict the noise level at any distance in the same model. The correctness of the model results is verified by comparison with the published numerical models, field measurements, and semi-analytical models. Although there are many studies[6–23] investigating the problem of pile driving noise, the advantages of this analytical model are obvious and the differences between this model and the previous methods are listed in Table I.

The structure of this paper is as follows. In Sec. II, the governing equations are given. In Sec. III, the governing equations are solved to obtain the results. In Sec. IV, the results are compared with those found in the literature. Finally, Sec. V gives an overview of the main conclusions of this paper.

II. MODEL DESCRIPTION AND GOVERNING EQUATIONS

A. Model description

The pile-fluid-soil coupling system is shown in Fig.1, and an axisymmetric model is established to reduce the computational effort. Two assumptions are used: (i) the fluid and soil consist of independent horizontal thin layers following Baranov–Novak's plane-strain model,[24] and (ii) the soil layers below the pile are simplified as a soil half-space. The impact force on the pile top is simplified as a known external load, $F(t)$.[13,22] The pipe pile is modelled as elastic and occupies the domain of $0 \leq z \leq L$ and $r_0 \leq r \leq r_1$. The seabed occupies the domain of $z \geq h_2$ and $r \leq r_0$ or $r \geq r_1$. r_0 is the inner radius of the pile, and r_1 is the outer radius of

the pile. The fluid layer is assumed to be an inviscid compressible medium with a pressure release boundary at $z = h_1$. It occupies the domain $h_1 \leq z \leq h_2$ and $r \leq r_0$ or $r \geq r_1$. The fluid depth is $H_w = h_2 - h_1$. The stresses acting on the pile-fluid and pile-soil surfaces are shown in Fig.1: p_{fi} and p_{fo} represent the fluid pressure inside and outside the pile, respectively. τ_{srzi} and τ_{srzo} represent the soil shear stress inside and outside the pile, respectively.

B. Governing equations

1. Governing equations of the soil

The soil governing equations can be considered by the plane-strain model, also known as the Baranov–Novak thin-layer model:[24]

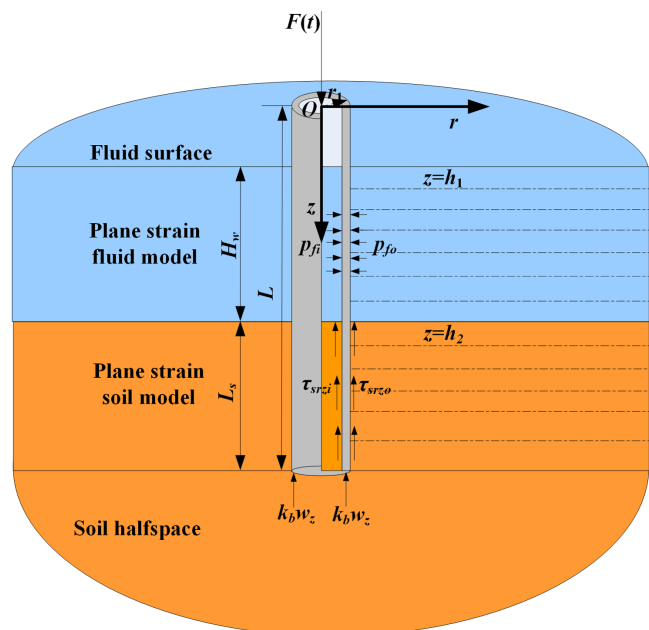$$G_s^* \frac{\partial^2 u}{\partial r^2} + G_s^* \frac{\partial u}{r \partial r} = \rho_s \ddot{u}, \tag{1}$$

FIG. 1. (Color online) Illustration of the model.

where $u(r, t)$ is the vertical soil displacement. ρ_s is the density of the soil. The dot (•) above the displacement vectors represents the derivative with respect to time t. $G_s^* = G_s(1 + 2\alpha_s i)$ is the complex Lamé constant of the soil. α_s is the hysteretic damping of the soil. The Lamé constant can be obtained from $G_s = E_s/2(1 + \nu_s)$, where E_s and ν_s are the elastic modulus and the Poisson's ratio of the soil, respectively.

2. Governing equations of the fluid

Similar to the Baranov–Novak thin-layer model used for soils, the governing equation for the fluid can be expressed in a cylindrical coordinate system as follows:

$$\frac{\partial^2 \varphi}{\partial r^2} + \frac{\partial \varphi}{r \partial r} = \frac{1}{c_F^2} \ddot{\varphi} . \tag{2}$$

Here, $\varphi(r, t)$ is the potential function of the fluid and c_F is the speeds of the fluid. The radial velocity v_{fr} and pressure p_f of the fluid are defined as $v_{fr} = (\partial \varphi / \partial r)$ and $p_f = -\rho_f \dot{\varphi}$, respectively. ρ_f is the density of the fluid.

3. Governing equations of the pile

To consider pile-fluid-soil interaction, the pile governing equations containing both radial and vertical displacements can be expressed as

$$G_p^* \nabla^2 \mathbf{w} + (\lambda_p^* + G_p^*) \nabla \nabla \cdot \mathbf{w} = \rho_p \ddot{\mathbf{w}}, \tag{3}$$

in which $\nabla^2 = (\partial/\partial r^2) + (1/r)(\partial/\partial r) + (\partial/\partial z^2)$ and $\mathbf{w} = [w_r(r, z, t), w_z(r, z, t)]^T$ is the displacement vector of the pile. ρ_p is the density of the pile. $\lambda_p^* = \lambda_p(1 + 2\alpha_p i)$ and $G_p^* = G_p(1 + 2\alpha_p i)$ are the complex Lamé constants of the pile. α_p is the hysteretic damping of the pile. The Lamé constants can be obtained from $G_p = E_p/2(1 + \nu_p)$ and $\lambda_p = 2G_p\nu_p/(1 - 2\nu_p)$, where E_p and ν_p are the elastic modulus and the Poisson's ratio of the pile, respectively.

C. Boundary conditions

To solve the governing equations, some boundary and interface conditions must be satisfied:

1. Boundary conditions of the fluid layer

$$\varphi_i|_{r \to 0} \neq \infty, \quad \varphi_o|_{r \to \infty} = 0, \quad p_f|_{z=h_1} = 0, \tag{4}$$

where φ_i and φ_o are the potential functions of the fluid inside and outside the pile, respectively. $z = h_1$ is the pressure release surface of the fluid.

2. Boundary conditions at the top of the pile at z = 0

$$\sigma_{pz}|_{z=0} = -F(t) \quad r_0 \leq r \leq r_1, \tag{5}$$

in which σ_{pz} is the vertical normal stress of the pile.

3. Boundary condition of the base of the pile at z = L

$$\sigma_{pz}A + k_b w_z|_{z=L} = 0, \tag{6}$$

where $k_b = \alpha_v 4G_b r_1/(1 - \nu_b)$ and $\alpha_v = 0.68$ (see Refs. [25] and [26]), and G_b and ν_b are the substratum soil's shear modules and Poisson ratio, respectively. The pile base area $A = \pi(r_1^2 - r_0^2)$. To simplify the calculation, the radial displacement of the pile is ignored under the pile base boundary condition.

4. The continuity conditions at the pile-fluid interface, assuming the non-slip behavior

For the inner surface of the pipe pile at $r = r_0$, $h_1 \leq z \leq h_2$:

$$v_{fri} = \dot{w}_r, \quad \tau_{prz} = 0, \quad p_{fi} = -\sigma_{pr}. \tag{7}$$

For the outer surface of the pipe pile at $r = r_1$, $h_1 \leq z \leq h_2$:

$$v_{fro} = \dot{w}_r, \quad \tau_{prz} = 0, \quad p_{fo} = -\sigma_{pr}, \tag{8}$$

where v_{fri}, v_{fro}, p_{fi}, and p_{fro} are the radial velocity and pressure of the fluid inside and outside the pile, respectively. σ_{pr} and τ_{prz} are the radial normal stress and shear stress of the pile, respectively.

5. The continuity conditions at the pile-soil interface, assuming the non-slip behavior

For the inner surface of the pipe pile at $r = r_0$, $h_2 \leq z \leq L$:

$$u_i = w_z, \quad \tau_{srzi} = \tau_{prz}, \quad \sigma_{pr} = 0. \tag{9}$$

For the outer surface of the pipe pile at $r = r_1$, $h_2 \leq z \leq L$:

$$u_o = w_z, \quad \tau_{srzo} = \tau_{prz}, \quad \sigma_{pr} = 0, \tag{10}$$

where u_i and u_o are the displacement of the soil inside and outside the pile, respectively.

6. Boundary conditions of the soil (natural boundary conditions)

$$u_i|_{r \to 0} \neq \infty, \quad u_o|_{r \to \infty} = 0. \tag{11}$$

7. Initial conditions for the pile-soil system (t = 0)

$$\varphi_i|_{t=0} = u_i|_{t=0} = \varphi_o|_{t=0} = u_o|_{t=0} = w_r|_{t=0} = w_z|_{t=0} = 0 \tag{12a}$$

$$\dot{\varphi}_i|_{t=0} = \dot{u}_i|_{t=0} = \dot{\varphi}_o|_{t=0} = \dot{u}_o|_{t=0} = \dot{w}_r|_{t=0} = \dot{w}_z|_{t=0} = 0. \tag{12b}$$

In addition, the displacement and velocity of the whole system are assumed to be zero at the initial time.

Rui He and Yongshan Song

III. THEORETICAL FORMULATION

In this subsection, the governing equations of soil, pile, and fluid are solved. Compared to Baranov–Novak's method,[24] both axial and radial displacement components of the pile as a function of frequency are considered and a finite fluid layer with dynamic pile-fluid-soil interaction is introduced.

A. Solutions of the soil governing equations

The Laplace transform is used to solve the soil governing equations. The one-sided Laplace transform and the inverse Laplace transform of a function, $f(t)$, are defined as follows:[26]

$$\bar{f}(s) = \int_0^\infty e^{-st} f(t)\,\mathrm{d}t, \quad f(t) = \frac{1}{2\pi\mathrm{i}} \int_{\sigma-\mathrm{i}\infty}^{\sigma+\mathrm{i}\infty} \bar{f}(s) e^{st}\,\mathrm{d}s. \quad (13)$$

Using the Laplace transform, Eq. (1) with the initial conditions is expressed as

$$G_s^* \frac{\partial^2 \bar{u}}{\partial r^2} + G_s^* \frac{\partial \bar{u}}{r \partial r} = \rho_s s^2 \bar{u}, \quad (14)$$

where s is the Laplace transform parameter with $s = \mathrm{i}\omega$, ω is the excitation frequency, and $\mathrm{i} = \sqrt{-1}$. Solving Eq. (14) and combining boundary conditions in Eqs. (11) and (12), the soil displacement can be obtained as

$$\bar{u}_i = A_1 I_0(\eta_s r), \quad \bar{u}_o = A_2 K_0(\eta_s r), \quad (15)$$

where A_1 and A_2 are undetermined coefficients and $\eta_s = \sqrt{\rho_s s^2 / G_s^*}$. $I_0(r)$ and $K_0(r)$ are modified Bessel functions.

B. Solutions of the pile governing equations

By using the Laplace transform, Eq. (3) can be converted to a frequency domain:

$$G_p^* \nabla^2 \bar{\mathbf{w}} + (\lambda_p^* + G_p^*) \nabla \nabla \cdot \bar{\mathbf{w}} = \rho_p s^2 \bar{\mathbf{w}}. \quad (16)$$

Using Helmholtz decomposition and the method of separation of variables,[24] the general solution of Eq. (16) can be obtained. Using the superposition principle, the non-homogeneous boundary condition at the pile top is converted to a special solution of $\bar{w}_z$ and a homogeneous condition:

$$\sigma_{pz}\big|_{z=0} = 0 \quad r_0 \leq r \leq r_1. \quad (17)$$

Substituting the general solution of $\bar{w}_z$ into Eqs. (17) and (6), the pile displacement can be obtained as

$$\bar{w}_r = \sum_{n=1}^{\infty} \Big[B_{1n}\eta_{pn} I_1(\eta_{pn}r) - B_{2n}\eta_{pn} K_1(\eta_{pn}r)$$
$$- B_{3n}\beta_{pn}\xi_{pn} I_1(\xi_{pn}r) + B_{4n}\beta_{pn}\xi_{pn} K_1(\xi_{pn}r) \Big] \sin(\beta_{pn}z), \quad (18a)$$

$$\bar{w}_z = \sum_{n=1}^{\infty} \Big[B_{1n}\beta_{pn} I_0(\eta_{pn}r) + B_{2n}\beta_{pn} K_0(\eta_{pn}r)$$
$$- B_{3n}\xi_{pn}^2 I_0(\xi_{pn}r) - B_{4n}\xi_{pn}^2 K_0(\xi_{pn}r) \Big] \cos(\beta_{pn}z) + \bar{w}_z^*, \quad (18b)$$

where $B_i, i = 1, 2, 3, 4$ are undetermined coefficients, $\eta_{pn} = \sqrt{\beta_{pn}^2 + \rho_p s^2/(\lambda_p^* + 2G_p^*)}$, and $\xi_{pn} = \sqrt{\beta_{pn}^2 + \rho_p s^2/G_p^*}$. β_{pn} can be obtained by solving the transcendental equation:

$$(\lambda_p^* + 2G_p^*)\big[-\beta_{pn}\sin(\beta_p L)\big] = -(k_b/A)\cos(\beta_{pn}L). \quad (19)$$

Substituting $\bar{w}_z^*$ into Eq. (16),

$$\frac{d^2 \bar{w}_z^*(z)}{dz^2} + \gamma^2 \bar{w}_z^*(z) = 0, \quad (20)$$

where $\gamma = \sqrt{-\rho_p s^2/(\lambda_p^* + 2G_p^*)}$. Solving Eq. (20) and combining boundary conditions in Eqs. (5) and (6), $\bar{w}_z^*$ is obtained as

$$\bar{w}_z^* = E_1 \cos(\gamma z) + E_2 \sin(\gamma z), \quad (21)$$

where

$$E_1 = \frac{-\bar{F}(s)}{(\lambda_p^* + 2G_p^*)\gamma}$$

and

$$E_2 = \frac{(\lambda_p^* + 2G_p^*)\gamma\cos(\gamma L) + (k_b/A)\sin(\gamma L)}{(\lambda_p^* + 2G_p^*)\gamma\sin(\gamma L) - (k_b/A)\cos(\gamma L)} E_1.$$

C. Solution of the fluid governing equations

Transform Eq. (2) into the frequency domain using the Laplace transform:

$$\frac{\partial^2 \bar{\varphi}}{\partial r^2} + \frac{\partial \bar{\varphi}}{r \partial r} - \frac{s^2}{c_F^2} \bar{\varphi} = 0. \quad (22)$$

Solving Eq. (22) and combining the boundary conditions of Eqs. (4), (7), and (8), the potential function of the fluid is derived as

$$\bar{\varphi}_i = \frac{s I_0(\zeta_j r)}{\zeta_j I_1(\zeta_j r_0)} \sum_{n=1}^{\infty} \Big[B_{1n}\eta_{pn} I_1(\eta_{pn}r) - B_{2n}\eta_{pn} K_1(\eta_{pn}r)$$
$$- B_{3n}\beta_{pn}\xi_{pn} I_1(\xi_{pn}r) + B_{4n}\beta_{pn}\xi_{pn} K_1(\xi_{pn}r) \Big] \sin(\beta_{pn}z), \quad (23a)$$

$$\bar{\varphi}_o = -\frac{s K_0(\zeta_j r)}{\zeta_j K_1(\zeta_j r_1)} \sum_{n=1}^{\infty} \Big[B_{1n}\eta_{pn} I_1(\eta_{pn}r) - B_{2n}\eta_{pn} K_1(\eta_{pn}r)$$
$$- B_{3n}\beta_{pn}\xi_{pn} I_1(\xi_{pn}r) + B_{4n}\beta_{pn}\xi_{pn} K_1(\xi_{pn}r) \Big] \sin(\beta_{pn}z), \quad (23b)$$
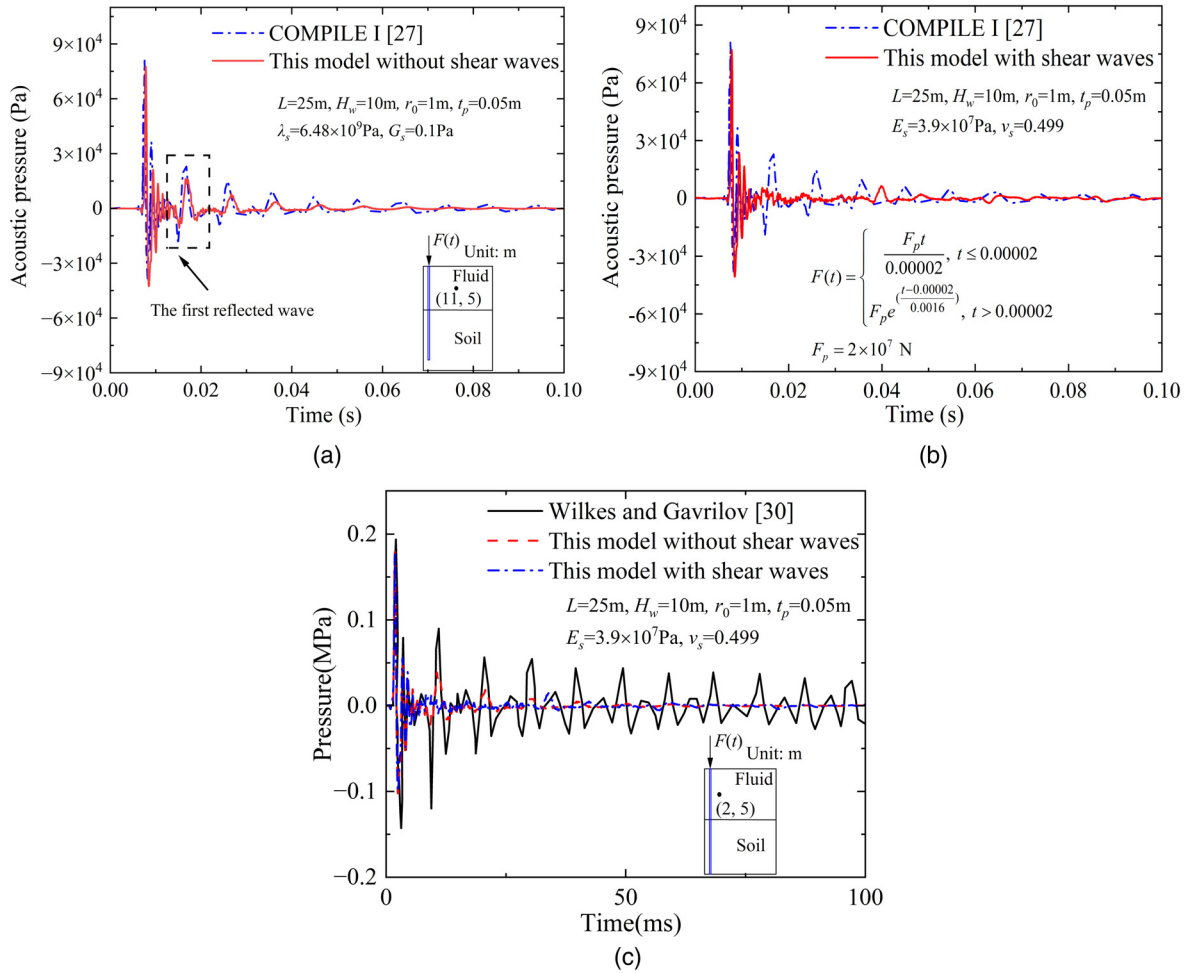
where $\zeta_j = \sqrt{s^2/c_F^2}$.

FIG. 2. (Color online) Comparison of the sound pressure with (a) comparison with COMPILE (Ref. 27); (b) comparison with COMPILE (Ref. 27); (c) comparison with Wilkes and Gavrilov (Ref. 30).

D. Derivation of the undetermined coefficients

Given the continuity of the pile-fluid-soil, and using the orthogonality of the trigonometric functions, the following equations are obtained to solve the indeterminate coefficients:

$$\int_{h_2}^{L} \bar{u}_i(r_0, z)\cos(\beta_{pn}z)\mathrm{d}z = \int_{h_2}^{L} \bar{w}_z(r_0, z)\cos(\beta_{pn}z)\mathrm{d}z, \quad (24)$$

$$\int_{h_2}^{L} \bar{\tau}_{srzi}(r_0, z)\cos(\beta_{pn}z)\mathrm{d}z = \int_{h_2}^{L} \bar{\tau}_{prz}(r_0, z)\cos(\beta_{pn}z)\mathrm{d}z, \quad (25)$$

$$\int_{h_1}^{h_2} s\rho_f\bar{\varphi}_i(r_0, z)\sin(\beta_{pn}z)\mathrm{d}z = \int_{h_1}^{h_2} \bar{\sigma}_{pr}(r_0, z)\sin(\beta_{pn}z)\mathrm{d}z, \quad (26)$$

$$\int_{h_2}^{L} \bar{u}_o(r_1, z)\cos(\beta_{pn}z)\mathrm{d}z = \int_{h_2}^{L} \bar{w}_z(r_1, z)\cos(\beta_{pn}z)\mathrm{d}z, \quad (27)$$

$$\int_{h_2}^{L} \bar{\tau}_{srzo}(r_1, z)\cos(\beta_{pn}z)\mathrm{d}z = \int_{h_2}^{L} \bar{\tau}_{prz}(r_1, z)\cos(\beta_{pn}z)\mathrm{d}z, \quad (28)$$

$$\int_{h_1}^{h_2} s\rho_f\bar{\varphi}_o(r_1, z)\sin(\beta_{pn}z)\mathrm{d}z = \int_{h_1}^{h_2} \bar{\sigma}_{pr}(r_1, z)\sin(\beta_{pn}z)\mathrm{d}z. \quad (29)$$

Substituting Eqs. (15), (18), (21), and (23) into Eqs. (24)–(29), a system of non-homogeneous linear equations is obtained and the undetermined coefficients can be solved.

IV. VALIDATION AND FURTHER ANALYSIS

In this section, this model will be verified by two benchmark numerical studies,[27,28] one semi-analytical solution,[22] and two measurement campaigns.[13,16] For the infinite summations in the calculation, the upper truncation limit of each model was determined by performing a convergence analysis of the models. For fairness, the same pile and soil parameters will be used, and for the modelling of multi-layered soils or piles, the parameters in this model are taken as the average value. Acoustic pressure, sound exposure level (SEL), and the peak sound pressure level (SPL) are compared in this section, where SEL is defined as[29]

$$\mathrm{SEL} = 10\log_{10}\left(\frac{1}{T_0}\int_{-\infty}^{\infty}\frac{p_f(t)^2}{p_0^2}\mathrm{d}t\right) \text{ dB re } 1\,\mu\mathrm{Pa}, \quad (30)$$

in which the reference pressure p_0 is equal to $1\,\mu\mathrm{Pa}$ and the reference time interval T_0 is equal to 1 s. The SPL is defined as[29]
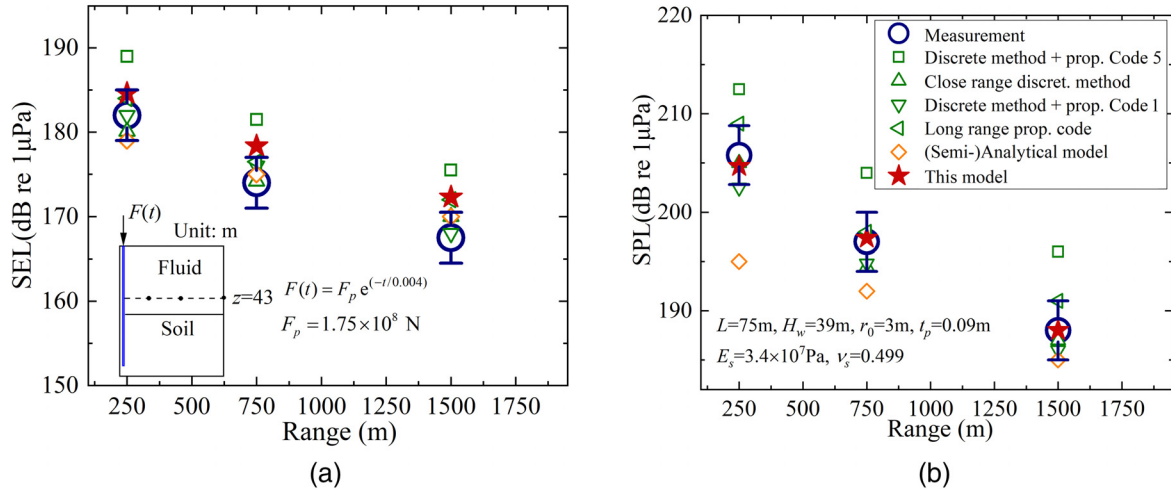
FIG. 3. (Color online) Comparison of the far-field acoustic pressure with COMPILE II (Ref. 28): (a) the sound exposure level (SEL); (b) the peak sound pressure level (SPL).

$$\text{SPL} = 10 \log_{10} \left(\frac{\max\left[|p_f(t)^2| \right]}{p_0^2} \right) \text{dB re } 1\,\mu\text{Pa.} \qquad (31)$$

A. Comparison with the benchmark project COMPILE I

Due to the lack of accurate analytical solutions to the problem of pile driving noise, the COMPILE workshop presented a detailed benchmark case to verify the accuracy of different computational models.[27] A brief outline of the impact force, pile, soil, and fluid parameters is shown in Fig. 2, while the details can be found in Ref. 27. The model established in this paper is consistent with the COMPILE benchmark case.

Figure 2(a) shows the results of the sound pressure in the fluid zone at the point located at $r = 11$, $z = 5$ m. The maximum pressure value calculated by the analytical model is about 78 kPa, which is well within the results (about 70–80 kPa) of seven other different numerical models.[27]

Reflected waves from the head and tip of the pile are also observed simultaneously, similar to other models. Furthermore, shear waves in the soil highly reduced the amplitude of the reflected waves (energy will transfer into the shear waves in the sediment[30]), as shown in Fig. 2(b). In addition, Wilkes and Gavrilov[30] also calculated the sound pressure at $r = 2$, $z = 5$ m: based on the COMPILE I benchmark case, the result is consistent with this model [Fig. 2(c)].

B. Comparison with the benchmark project COMPILE II

To verify the effectiveness of the model in predicting the far-field underwater noise, the model is compared to another benchmark scenario provided by COMPILE II.[28] The sampling points are located at distances $r = 250$, 750, and 1500 m from the pile center, 2 m above the seafloor. The parameters used in this model are shown in Fig. 3. To simplify the model in this paper, the pile is assumed to be a cylindrical shell with an average diameter of 6 m. The soil layers are simplified as a homogeneous layer whose Young's modulus is the average of
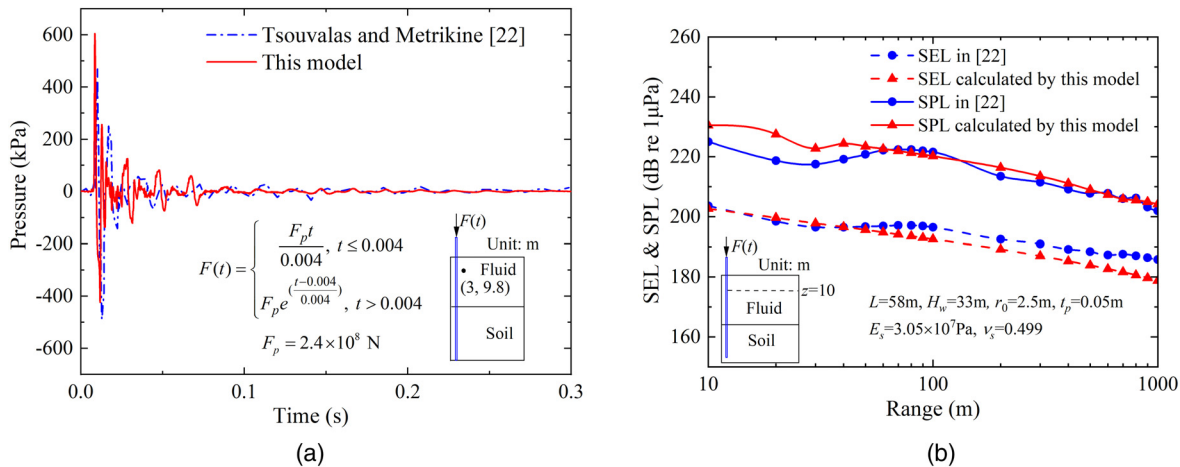

FIG. 4. (Color online) Comparisons with Tsouvalas and Metrikine (Ref. 22): (a) sound pressure at a point, $r = 3$ m, $z = 9.8$ m; (b) SEL and SPL at the plane $z = 10$ m.
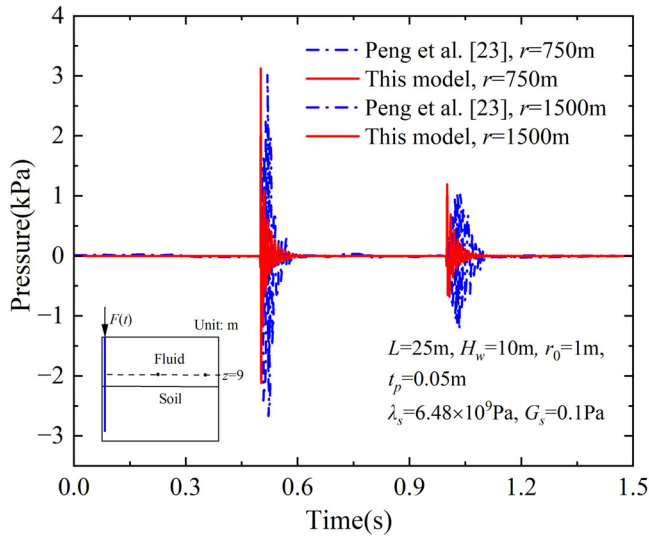
FIG. 5. (Color online) Comparisons with Peng *et al.* (Ref. 23): sound pressure at various distances above 1 m from the seabed.

all soil layers along the pile. The predicted results are compared with the predictions of five other groups and the measured data. The predicted results of this model are found to be in good agreement with the measured data, which have a typical measurement uncertainty of 3 dB.

C. Comparison with a semi-analytical model

Large-diameter monopiles are commonly used in recent engineering applications. Tsouvalas and Metrikine[22] proposed a semi-analytical model to predict the underwater noise caused by monopile driving. In this section, the proposed analytical model is compared to Ref. 22 with the same parameters and impact force.

The comparisons of the results obtained by the two models are shown in Fig. 4. It can be seen that the maximum values of the sound pressure [Fig. 4(a)], the SEL, and the peak SPL [Fig. 4(b)] are close in the two models, while the sound pressure calculated by this model is somehow higher than the results of Tsouvalas and Metrikine. The differences may come from (i) different boundary conditions at the base

of the pile, (ii) the different governing equations of the pile and soil, and (iii) the averaged soil modulus of Ref. 22 along the pile, which is used here.

On the other hand, Peng *et al.*[23] proposed a two-step modeling approach to predict the far-field noise caused by pile driving. Based on the previous benchmark case parameters provided by COMPILE I, the sound pressures in the time domain at distances of 750 and 1500 m from the pile, above 1 m from the seabed, are shown in Fig. 5. Compared with the result provided by Peng *et al.*,[23] the time evolution of the pressure is in good agreement.

D. Comparison with field measurement at the Vashon Island Ferry Terminal

The field measurement campaign[13] was carried out at the Washington State Ferry, Vashon Island Ferry Terminal, where the pressure time series of the underwater noise was obtained at a range of 12 m using a vertical line array (VLA) of hydrophones. In fact, Reinhall and Dahl[13] have established a FEM model to predict underwater noise and the same parameters are also used in this comparison.

Figure 6 shows the comparison of the SPLs at two locations obtained by the analytical model and the measured data. It can be found that the maximum acoustic pressures calculated in this paper compare fairly well with the measured data, as the maximum noise is always the main focus for noise evaluation.

E. Comparison with field measurement at the BARD Offshore site

The field measurement in the German North Sea is used for comparison in this section. The elastic modulus of the soil is derived from the compressional wave velocity. The pile, fluid, and soil parameters are similar to those of Ref. 16.

Third-octave band levels refer to the mean value of the sound pressure in the corresponding octave band. Third-octave band levels are used in Ref. 16 and are considered to be more reasonable for acoustic assessment than spectral density levels. Thus, the third-octave band sound levels in
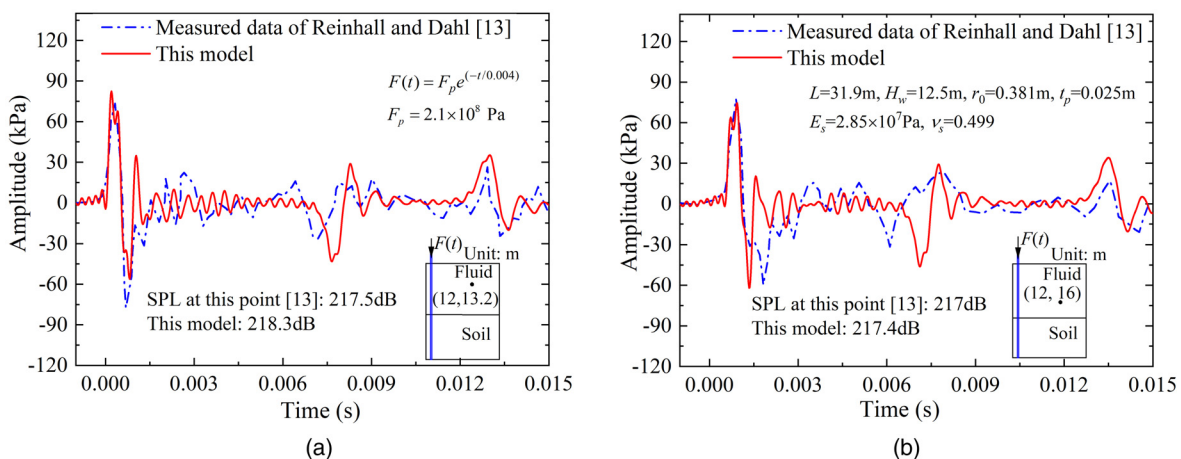

(a)

(b)

FIG. 6. (Color online) Comparison of the sound pressure with Reinhall and Dahl (Ref. 13): (a) 4.8 m off the bottom; (b) 2 m off the bottom.
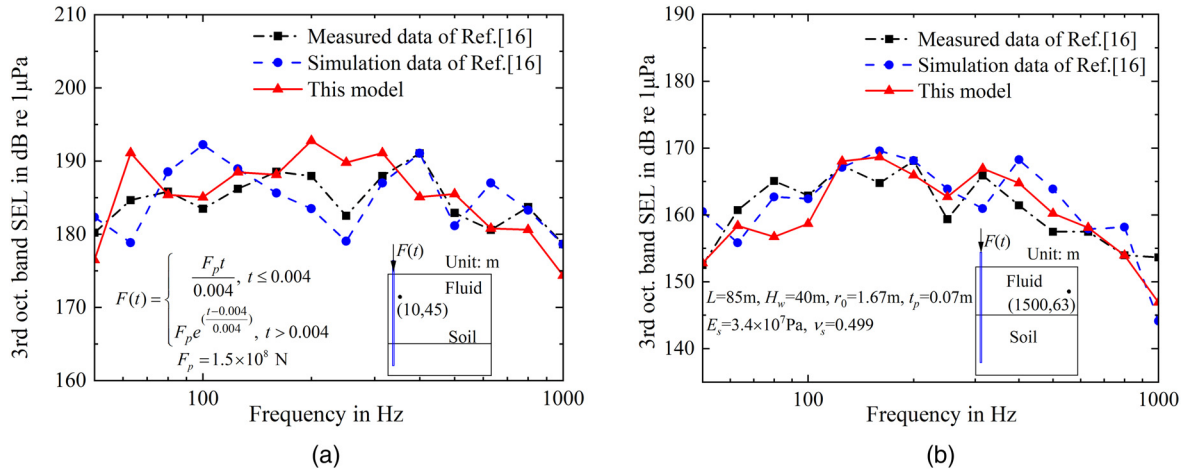
FIG. 7. (Color online) Comparison of the third-octave band sound exposure level with Fricke and Rolfes (Ref. 16): (a) near-field results; (b) far-field results.

the near field (10 m from the pile) and far field (1500 m from the pile) are compared in Fig. 7. The overall trend and the values are quite close, considering the uncertainties in the hammer impact force and the soil parameters. The difference in the maximum value of SEL in the near field is only about 3 dB [Fig.7(a)]. In the far field, the third-octave band SEL obtained from the analytical model and the measured data are quite close, although there are some differences in the detailed distribution along the frequency bands. Both Fricke and Rolfes[16] and other papers[31] pointed out that geo-acoustic modeling introduces a high degree of uncertainty in underwater noise prediction and cannot be avoided. Thus, the difference in the low frequency range is generally acceptable and it indicates again that the analytical solution is effective for predicting the noise levels in both the near field and far field.

F. Computational efficiency

Computational efficiency is very important for a model. The time required by a computer [Intel Core i9-13900 central processing unit (CPU) @3.00 GHz processor and 64 GB random access memory (RAM); Intel, Santa Clara, CA] to calculate the sound pressure at the point 500 m away from the pile using the proposed model is approximately 40 s. As the required computing time is not always available in the verification cases presented above, a FEM model[17] is modelled for comparison. The length of the modelled soil section is 500 m from the pile, while the parameters for the pile and water are similar to those in COMPILE I.[26] The time required by the same computer is about 20 h, which is about 1800 times more than for the analytical model. Furthermore, the time required increases dramatically with the increase in the soil area in the FEM model.

V. CONCLUSIONS

In this paper, a simplified semi-analytical model is established by extending the Baranov–Novak thin-layer

soil-structure interaction model to the subject of underwater noise prediction during pile driving by considering structure-fluid-soil interaction. It provides a preliminary and rapid prediction of the underwater noise of pile driving in both near field and far field in a single model, and the efficiency of the calculation is about 3 orders of magnitude higher than that of the FEM. The prediction results of the model are generally in good agreement with the well-documented cases. When comparing the near-field sound pressure in the time domain, the maximum sound pressure and wave arrival time calculated by this model are in good agreement with the numerical model, the semi-analytical model, and even the field measurement. In addition, the model has the same accuracy as other models in predicting pile driving noise in the far field and has an error of 3–10 dB re 1 μPa compared to the field measurement, which may be mainly due to the uncertainty in the far-field seabed topography, soil conditions, and bathymetric distributions. The model can be further extended to account for the effects of different soil conditions: e.g., porous soils with pore pressures, soil non-linearities, etc.

AUTHOR DECLARATIONS
Conflict of Interest

The authors have no conflicts to disclose.

DATA AVAILABILITY

The data that support the findings of this study are available from the corresponding author upon reasonable request.

[1]H. Bailey, B. Senior, D. Simmons, J. Rusin, G. Picken, and P. M. Thompson, "Assessing underwater noise levels during pile-driving at an offshore wind farm and its potential effects on marine mammals," Mar. Pollut. Bull. 60(6), 888–897 (2010).

[2]P. H. Dahl, C. A. F. de Jong, and A. N. Popper, "The underwater sound field from impact pile driving and its potential effects on marine life," Acoust. Today 11(2), 18–25 (2015).

[3]U. Stöber and F. Thomsen, "Effect of impact pile driving noise on marine mammals: A comparison of different noise exposure criteria," J. Acoust. Soc. Am. 145(5), 3252–3259 (2019).

[4]G. Hastie, N. D. Merchant, T. Götz, D. J. F. Russell, P. Thompson, and V. M. Janik, "Effects of impulsive noise on marine mammals: Investigating range-dependent risk," Ecol. Appl. 29(5), e01906 (2019).

[5]S. P. Robinson, P. D. Theobald, and P. A. Lepper, "Underwater noise generated from marine piling," Proc. Mtgs. Acoust. 17(1), 070080 (2012).

[6]P. H. Dahl and D. R. Dall'Osto, "On the underwater sound field from impact pile driving: Arrival structure, precursor arrivals, and energy streamlines," J. Acoust. Soc. Am. 142(2), 1141–1155 (2017).

[7]M. Zampolli, M. J. J. Nijhof, C. A. F. de Jong, M. A. Ainslie, E. H. W. Jansen, and B. A. J. Quesson, "Validation of finite element computations for the quantitative prediction of underwater noise from impact pile driving," J. Acoust. Soc. Am. 133(1), 72–81 (2013).

[8]A. MacGillivray, "Finite difference computational modelling of marine impact pile driving," J. Acoust. Soc. Am. 136, 2206 (2014).

[9]H. Kim, G. R. Potty, J. H. Miller, K. B. Smith, and G. Dossot, "Long range propagation modeling of offshore wind turbine noise using finite element and parabolic equation models," J. Acoust. Soc. Am. 131(4), 3392 (2012).

[10]J. Park, W. Seong, and K. Lee, "Modeling of underwater noise from pile driving using coupled finite element and parabolic equation model with improved parabolic equation starting field," J. Acoust. Soc. Am. 134(5), 4114 (2013).

[11]T. Lippert and S. Lippert, "Modelling of pile driving noise by means of wavenumber integration," Acoust. Aust. 40(3), 178–182 (2012).

[12]D. R. Wilkes, T. P. Gourlay, and A. N. Gavrilov, "Numerical modeling of radiated sound for impact pile driving in offshore environments," IEEE J. Ocean. Eng. 41(4), 1072–1078 (2016).

[13]P. G. Reinhall and P. H. Dahl, "Underwater Mach wave radiation from impact pile driving: Theory and observation," J. Acoust. Soc. Am. 130(3), 1209–1216 (2011).

[14]T. Lippert and O. von Estorff, "The significance of parameter uncertainties for the prediction of offshore pile driving noise," J. Acoust. Soc. Am. 136(5), 2463–2471 (2014).

[15]R. A. Hazelwood, P. C. Macey, S. P. Robinson, and L. S. Wang, "Optimal transmission of interface vibration wavelets—A simulation of seabed seismic responses," J. Mar. Sci. Eng. 6(2), 61 (2018).

[16]M. B. Fricke and R. Rolfes, "Towards a complete physically based forecast model for underwater noise related to impact pile driving," J. Acoust. Soc. Am. 137(3), 1564–1575 (2015).

[17]R. He, Y. Xiang, and Z. Guo, "A poroelastic model for near-field underwater noise caused by offshore monopile driving," J. Sound Vib. 564, 117878 (2023).

[18]M. V. Hall, "A semi-analytical model for non-Mach peak pressure of underwater acoustic pulses from offshore pile driving," Acoust. Aust 41, 42–51 (2013).

[19]A. Tsouvalas and A. V. Metrikine, "A semi-analytical model for the prediction of underwater noise from offshore pile driving," J. Sound Vib 332(13), 3232–3257 (2013).

[20]Q. Deng, W. Jiang, M. Tan, and J. T. Xing, "Modeling of offshore pile driving noise using a semi-analytical variational formulation," Appl. Acoust. 104, 85–100 (2016).

[21]A. Tsouvalas and A. V. Metrikine, "A three-dimensional vibroacoustic model for the prediction of underwater noise from offshore pile driving," J. Sound Vib. 333(8), 2283–2311 (2014).

[22]A. Tsouvalas and A. V. Metrikine, "Structure-borne wave radiation by impact and vibratory piling in offshore installations: From sound prediction to auditory damage," J. Mar. Sci. Eng. 4(3), 44 (2016).

[23]Y. Peng, A. Tsouvalas, T. Stampoultzoglou, and A. Metrikine, "A fast computational model for near- and far-field noise prediction due to offshore pile driving," J. Acoust. Soc. Am. 149(3), 1772–1790 (2021).

[24]M. Novak, "Dynamic stiffness and damping of piles," Can. Geotech. J. 11, 574–598 (1974).

[25]R. He, X. Bai, W. Peng, and J. Zhang, "Dynamic impedances of ring disks buried in arbitrary depths," Eur. J. Environ. Civil Eng. 26(15), 7664–7684 (2022).

[26]G. Militano and R. K. N. D. Rajapakse, "Dynamic response of a pile in a multi-layered soil to transient torsional and axial loading," Geotechnique 49(1), 91–109 (1999).

[27]S. Lippert, M. Nijhof, T. Lippert, D. Wilkes, A. Gavrilov, K. Heitmann, M. Ruhnau, O. von Estorff, A. Schäfke, I. Schäfer, J. Ehrlich, A. MacGillivray, J. Park, W. Seong, M. A. Ainslie, C. de Jong, M. Wood, L. Wang, and P. Theobald, "COMPILE—A generic benchmark case for predictions of marine pile-driving noise," IEEE J. Ocean. Eng. 41(4), 1061–1071 (2016).

[28]S. Lippert, O. Von Estorff, M. J. J. Nijhof, and T. Lippert, "COMPILE II—A benchmark of pile driving noise models against offshore measurements," in INTER-NOISE 2018—47th International Congress and Exposition on Noise Control Engineering: Impact of Noise Control Engineering, Chicago, IL (August 25–28, 2018).

[29]M. A. Ainslie, M. B. Halvorsen, and S. P. Robinson, "A terminology standard for underwater acoustics and the benefits of international standardization," IEEE J. Ocean. Eng. 47(1), 179–200 (2022).

[30]D. R. Wilkes and A. Gavrilov, "Numerical modelling of sound radiation from marine pile driving over elastic seabeds," in Lecture Notes in Mechanical Engineering (Springer, New York, 2016), pp. 107–112.

[31]T. Bohne, T. Grießmann, and R. Rolfes, "Comprehensive analysis of the seismic wave fields generated by offshore pile driving: A case study at the BARD Offshore 1 offshore wind farm," J. Acoust. Soc. Am. 155(3), 1856–1867 (2024).

782   J. Acoust. Soc. Am. 156 (2), August 2024

Rui He and Yongshan Song